

시분할 다중접속 방식의 위성통신 시스템을 위한 주파수 추정

정희원 김 중 문*, 종신회원 이 용 환*

Estimation of Frequency Offset in TDMA-Based Satellite Systems

Jong-Moon Kim* *Regular Member*, Yong-Hwan Lee* *Lifelong Member*

요 약

TDMA 시스템에서 신호를 수신하기 위해서는 정확한 주파수 및 시간 동기가 필요하다. 본 논문에서는 QPSK 신호를 전송하는 TDMA 방식의 위성통신 시스템에서 혼란 신호 없이 주파수 편이를 추정하는 방법을 제안한다. 제안된 방법은 수신 신호의 두 부분에서 정확도가 높게 위상을 추정하고, 이 위상 차이로부터 주파수 편이를 추정함으로써 기존의 주파수 편이 추정 방법과 비슷한 성능을 보이면서 적은 연산량이 요구된다. 제안된 방법을 GSM을 기반으로 확장된 GMR 위성통신 시스템에 적용하고 시뮬레이션을 통해 성능을 검증한다.

Key Words : GMR, satellite system, TDMA, carrier recovery, frequency offset

ABSTRACT

It is required for correct signal detection to accurately maintain the synchronization of frequency and timing in a TDMA system. In this paper, we consider nondecision-aided estimation of frequency offset for the transmission of QPSK signal in a TDMA-based satellite system. The proposed scheme estimates the phases of two parts in the burst and then estimates the frequency offset based on the difference between the two estimated phases. Thus, it can provides performance comparable to that of conventional schemes, while significantly reducing the implementation complexity. The performance of the proposed scheme is analyzed and verified by computer simulation, when applied to a GSM based geostationary earth orbit mobile radio(GMR) system.

I. Introduction

Time division multiple access techniques have widely been applied to satellite links and wireless communications^[1]. Reliable data detection in time division multiplexing access(TDMA) communication systems strictly requires the synchronization of carrier frequency/phase and symbol timing. TDMA systems such as GSM or geostationary earth orbit

mobile radio(GMR) impose stringent requirements on the frequency stability of receive oscillator because the frequency and timing of the received signal are used as the reference for the transmission of signal^[2,3].

A number of works have been proposed for the carrier recovery^[4-7]. Most of the previous works considered to the transmission of linearly modulated, burst-mode signal over additive white

* LG전자 DTV연구소 (jmoon13@lge.com), 서울대학교 전기공학부 송수신기술연구실 (ylee@snu.ac.kr)
논문번호 : KICS2005-10-428, 접수일자 : 2005년 10월 21일, 최종논문접수일자 : 2006년 3월 28일

gaussian noise (AWGN) channel with/without the use of training signal. The former schemes are called data-aided (DA) estimation^[5,6] and the latter schemes are called nondecision-aided (NDA) estimation^[7,8].

A maximum-likelihood (ML) scheme was proposed for PSK signals^[4], whereby a periodic training sequence is recursively passed through a bank of bandpass filters implemented in a form of discrete Fourier transform. It adjusts the frequency spacing so as to accurately estimate the frequency of spectrum peaks of the input signal, but it requires a large implementation complexity. To alleviate the implementation problem, simplified schemes were proposed by approximating the weight of the autocorrelation function in the likelihood equation^[5,6].

As an NDA scheme, a sequence of samples is obtained using differential symbol estimates that cancel out the QPSK data modulation from the received signal^[7]. The average phase slope of this sequence is proportional to the frequency offset in QPSK signal. The cited phase slope is evaluated and analyzed by a means of fitting technique^[8].

In a TDMA communication system, a unique codeword is often inserted in the burst for the detection of logical channel, timing synchronization and frequency synchronization. It would be desirable to avoid the use of a long codeword particularly when the transmission rate is low. The GMR specification suggests the insertion of a short codeword in each 5ms length burst for spectral efficiency. It is required to use an NDA frequency offset estimation scheme for frequency synchronization in the GMR system.

The performance of NDA frequency offset estimation schemes can be improved using a modified DA technique, but it requires a large implementation complexity. Thus, to alleviate the implementation problem, we propose an NDA scheme for the estimation of frequency offset while providing error performance comparable to that of the improved NDA schemes.

Following Introduction, Section II describes the proposed frequency offset estimation scheme and analyzes the performance. The performance of the

proposed scheme is evaluated when applied to the GMR system in Section III. Finally, conclusions are summarized in Section IV.

II. Frequency offset estimation

We consider the transmission of QPSK signal over an additive white Gaussian noise(AWGN) channel. Then, the output of the matched filter can be represented as

$$r_i = c_i \exp\{j(2\pi\Delta f T i + \phi)\} + n_i, \quad 0 \leq i < L \quad (1)$$

where c_i is QPSK symbol whose absolute value is the unit, Δf denotes the frequency offset, T is the symbol duration, ϕ is the carrier phase, L is the burst length represented in terms of symbols, and n_i is circular symmetric zero-mean complex Gaussian noise. The variance of the real and imaginary part of n_i is σ^2 and the signal-to-noise ratio (SNR) is defined as $\rho = 1/2\sigma^2$.

2.1 Conventional frequency offset estimation schemes

The frequency offset can be estimated in an NDA scheme using a 4-th order power function as^[7]

$$\hat{\Delta f} = \frac{1}{4 \cdot 2\pi T} \arg \left\{ \sum_{m=1}^L r_m^4 (r_{m-1}^4)^* \right\} \quad (2)$$

where $\arg\{z\}$ denotes the argument of a complex z taken in the interval $[-\pi, \pi]$. This scheme estimates the frequency offset by accumulating the phase difference between the symbols in the burst. It can provide a large operating range of $|\Delta f| < [8T]^{-1}$, but it may not provide good performance. Assuming that the frequency offset is unchanged within the burst, the frequency offset can be estimated by a linear increment of symbol phase as^[8]

$$\hat{\Delta f} = \left(\sum_{-N}^N i\alpha_{i+N} \right) / \left(8\pi T \sum_{-N}^N i^2 \right) = \left(3 \sum_{-N}^N i\alpha_{i+N} \right) / \left[2\pi T L(L^2 - 1) \right] \quad (3)$$

where $N = (L-1)/2$ and $\alpha_i = 4\arg(r_i) \bmod 2\pi$. The variance of the estimation error is given by

$$\sigma_{\Delta f}^2 \approx 3[\pi^2 T^2 L(L^2 - 1)/\sigma^2]. \quad (4)$$

This scheme somewhat improves the estimation but it still needs further improvement.

DA frequency offset estimation techniques can be applied to NDA frequency offset estimation schemes. Assuming that r_k is the received training signals, the frequency offset can be estimated by approximating the weight of the autocorrelation function in the likelihood equation^[5]

$$\Delta \hat{f} = \frac{\sum_{m=1}^M \arg\{\hat{R}_N(m)\}}{2\pi T \sum_{m=1}^M m} \quad (5)$$

where $\hat{R}_N(m) = \sum_{k=m}^{L-m} r_k (r_{k-m})^*$. If r_k is a QPSK modulated, (5) can be modified for NDA estimation as

$$\Delta \hat{f} = \frac{\sum_{m=1}^M \arg\{\tilde{R}_N(m)\}}{4 \cdot 2\pi T \sum_{m=1}^M m} \quad (6)$$

where $\tilde{R}_N(m) = \sum_{k=m}^{L-m} r_k^4 (r_{k-m}^4)^*$. Here, a 4-th order approximation is employed for the calculation of autocorrelation function while eliminating QPSK modulation. Thus, the phase difference in the autocorrelation function corresponds to four times of the actual phase difference. Another DA estimation scheme was proposed to reduce the implementation complexity^[6]. The frequency offset can be estimated by using a rectangular windowing function instead a parabolic one for the autocorrelation function in the likelihood equation as^[6]

$$\Delta \hat{f} = \frac{1}{\pi T(M+1)} \arg\left\{\sum_{k=1}^M R(k)\right\} \quad (7)$$

where $R(k) \square \sum_{i=k+1}^L r_i (r_{i-k})^* / (L-k)$. If r_k QPSK modulated, (7) can be modified for NDA estimation as

$$\Delta \hat{f} = \frac{1}{4\pi T(M+1)} \arg\left\{\sum_{k=1}^M \tilde{R}(k)\right\} \quad (8)$$

where $\tilde{R}(k) \square \sum_{i=k+1}^L r_i^4 (r_{i-k}^4)^* / (L-k)$.

These modified DA schemes for the NDA estimation can provide good error performance at the expense of large implementation complexity for the calculation of autocorrelation function.

2.2. Proposed frequency offset estimation scheme

The frequency offset can be estimated from the difference of two phases as

$$\Delta \hat{f} = \frac{1}{4 \cdot 2\pi DT} \arg\left\{\left(\sum_{m=K}^{K+N} r_{m+D}^4\right) \cdot \left(\sum_{m=K}^{K+N} r_m^4\right)^*\right\} \quad (9)$$

where K represents the start point of the symbols used for the estimation, D denotes the distance between the two part of the burst, N denotes the summation length for each part and

$$L = 2K + N + D \quad (10)$$

The variable K can be set zero to maximally use the symbols for the estimation. It can be seen from (9) that the operating range of the proposed scheme is $|\Delta f| < [8DT]^{-1}$.

For the analysis of performance, the received signal can be represented using a 4-th order function as

$$\begin{aligned} r_i^4 &= [c_i e^{j(2\pi\Delta f T i + \theta)} + n_i]^4 \\ &= s_i^4 + 4s_i^3 n_i + 6s_i^2 n_i^2 + 4s_i n_i^3 + n_i^4 \end{aligned} \quad (11)$$

where

$$s_i = c_i e^{j(2\pi\Delta f T i + \theta)} \quad (12)$$

Here, s_i^4 is the desired term for the estimation of frequency offset and the remaining terms are noise. Defining the noise term as

$$w_i \square 4s_i^3 n_i + 6s_i^2 n_i^2 + 4s_i n_i^3 + n_i^4 \quad (13)$$

it can be shown that

$$\begin{aligned} E\{w_i\} &= 0 \\ E\{\text{Re}\{w_i\} \cdot \text{Im}\{w_i\}\} &= E\{\text{Re}\{w_i\}\} E\{\text{Im}\{w_i\}\} = 0 \\ \sigma_w^2 = \text{var}[w_i] &= 32\sigma^2 + 288\sigma^4 + 768\sigma^6 + 384\sigma^8 \\ \text{var}[\text{Re}\{w_i\}] &= \text{var}[\text{Im}\{w_i\}] = \sigma_w^2 / 2 \end{aligned} \quad (14)$$

Thus, w_i is a circular symmetric zero-mean complex random variable with variance σ_w^2 . The error variance $E\left\{\left(\Delta\hat{f} - \Delta f\right)^2\right\}$ of the estimator (9) can be calculated when $\rho \ll 1$ and $8\pi\Delta f TN \ll 1$.

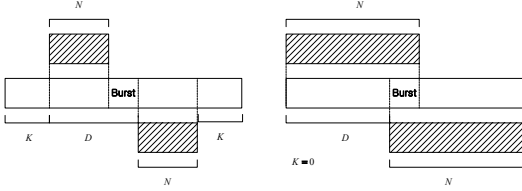


Fig. 1. Structure of the proposed estimation scheme

Letting

$$\xi \triangleq e^{j8\pi\Delta f TD} \quad (15)$$

$$\hat{\xi} \triangleq e^{j8\pi\Delta f TD} = \left(\sum_{m=1}^N r_{m+L}^4 \right) \cdot \left(\sum_{m=1}^N r_m^4 \right)^* \quad (16)$$

$$\varepsilon \triangleq 8\pi \left(\Delta\hat{f} - \Delta f \right) TD \quad (17)$$

(9) can be written as

$$E\left\{\left(\Delta\hat{f} - \Delta f\right)^2\right\} = \frac{1}{(8\pi TD)^2} E\left\{\varepsilon^2\right\} \quad (18)$$

where

$$\varepsilon = \arg\left\{\frac{\hat{\xi}}{\xi}\right\} = \arg\left\{\left(\sum_{m=1}^N r_{m+L}^4\right) \cdot \left(\sum_{m=1}^N r_m^4\right)^* \xi^*\right\} \quad (19)$$

Letting $\omega_o \triangleq 4 \cdot 2\pi\Delta f T$ and $\Delta\phi \triangleq 4 \cdot 2\pi\Delta f TD$, it can be shown that

$$\begin{aligned} \varepsilon &= \arg\left\{e^{j\Delta\phi} + w_{D+1} + e^{j(\omega_o + \Delta\phi)} + w_{D+2} + \dots + e^{j(\omega_o(M-1) + \Delta\phi)} + w_{D+N}\right\} \\ &\quad \cdot \left(e^{-j0} + w_1^* + e^{-j\omega_o} + w_2^* + \dots + e^{-j\omega_o(M-1)} + w_N^*\right) \cdot e^{-j\Delta\phi} \\ &= \arg\left\{\left(N + 2 \sum_{m=1}^{N-1} (N-m) \cos(m\omega_o)\right) + e^{j(N-1)\omega_o/2} \frac{\sin(N\omega_o/2)}{\sin(\omega_o/2)} \sum_{i=1}^N w_i^*\right. \\ &\quad \left.+ e^{-j(N-1)\omega_o/2} \frac{\sin(N\omega_o/2)}{\sin(\omega_o/2)} \sum_{i=1}^N w_{i+D} + \sum_{i=1}^N \sum_{j=1}^N w_{i+D} w_j^*\right\} \\ &\cong \frac{1}{\left(N + 2 \sum_{m=1}^{N-1} (N-m) \cos(m\omega_o)\right)} \cdot \text{Im}\left\{e^{j(N-1)\omega_o/2} \frac{\sin(N\omega_o/2)}{\sin(\omega_o/2)} \sum_{i=1}^N w_i^*\right. \\ &\quad \left.+ e^{-j(N-1)\omega_o/2} \frac{\sin(N\omega_o/2)}{\sin(\omega_o/2)} \sum_{i=1}^N w_{i+D} + \sum_{i=1}^N \sum_{j=1}^N w_{i+D} w_j^*\right\} \quad (20) \end{aligned}$$

Since high SNR assumed, $w_{i+D} w_j^*$ terms can be neglected. If $D \geq N$, random variable w_i are independent identically distributed (i.i.d) with characteristics (14). Thus, it can be shown that

$$E\left\{\varepsilon^2\right\} \cong \frac{N\sigma_w^2 \sin^2(N\omega_o/2) / \sin^2(\omega_o/2)}{\left(N + 2 \sum_{m=1}^{M-1} (N-m) \cos(m\omega_o)\right)^2} \quad (21)$$

On the other hand, if $D < N$, the $(N-D)$ terms of $e^{j(N-1)\omega_o/2} \sum_{i=1}^N w_i^*$ and $e^{-j(N-1)\omega_o/2} \sum_{i=1}^N w_{i+D}$ in (20) are overlapped as shown in Fig 1. Because each of overlapped terms is complex conjugate, it has zero imaginary part. Since the remaining $\{w_i\}$ terms are i.i.d., it can be shown that

$$E\left\{\varepsilon^2\right\} \cong \frac{D\sigma_w^2 \sin^2(N\omega_o/2) / \sin^2(\omega_o/2)}{\left(N + 2 \sum_{m=1}^{M-1} (N-m) \cos(m\omega_o)\right)^2} \quad (22)$$

From (18), (21) and (22), we get

$$E\left\{\left(\Delta\hat{f} - \Delta f\right)^2\right\} \cong \frac{1}{(8\pi TD)^2} \frac{\min(N,D)\sigma_w^2 \sin^2(8\pi\Delta f TN/2) / \sin^2(8\pi\Delta f T/2)}{\left(N + 2 \sum_{m=1}^{M-1} (N-m) \cos(8\pi\Delta f Tm)\right)^2} \quad (23)$$

where $\min(A,B)$ denotes the minimum of A and B. It can be seen that the error variance is related to the frequency offset Δf .

On the other hand, when $8\pi\Delta f TN \ll 1$, we have

$$\left[\frac{\sin(8\pi\Delta f TN/2)}{\sin(8\pi\Delta f T/2)}\right]^2 \cong N^2 \quad (24)$$

Thus,

$$\begin{aligned} E\left\{\left(\Delta\hat{f} - \Delta f\right)^2\right\} &\cong \frac{1}{(8\pi TD)^2} \frac{\min(N,D)\sigma_w^2}{N^2} \\ &= \frac{\min(N,D)}{8(\pi TND)^2} \cdot \left(\frac{2}{\rho} + \frac{9}{\rho^2} + \frac{12}{\rho^3} + \frac{3}{\rho^4}\right) \quad (25) \end{aligned}$$

Fig. 2 depicts the normalized error variance $(\sigma_{\varepsilon} T_s)^2$ as a function of ρ when $L=112$, $K=0$, and $\Delta f=0$. Solid lines represent the error variance (25), while the symbols denote the simulation results. It can be seen that the analysis and simulation result agree well unless the SNR

is very low.

Fig. 3 depicts the normalized error variance as a function of N for three different values of SNR. By differentiating (25) with respect to N , the optimum values of N are $L/3$ and $2L/3$. The use of $N=2L/3$ provides an operating range wider than the use of $N=L/3$ at the expense of computational complexity. In what follows, we consider the use of $N=2L/3$ unless stated explicitly.

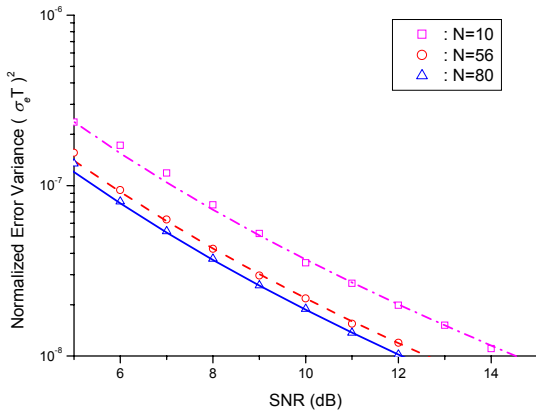


Fig. 2. Performance of the proposed estimation scheme

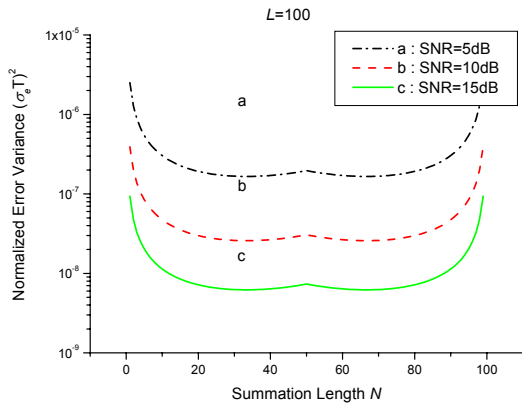
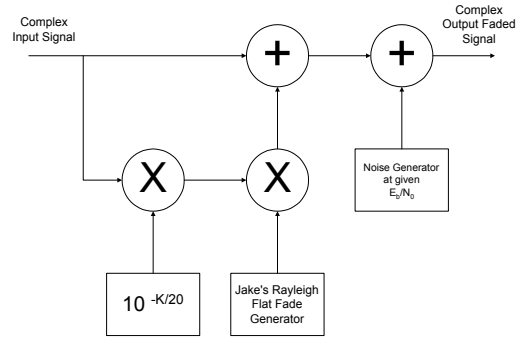


Fig. 3. Dependence on N of the estimator performance

III. Performance evaluation

Fig. 4 shows a Rician channel model given by the GMR specification. Then, the output of the matched filter can be represented as

$$r_i = c_i a_i \exp\{j(2\pi\Delta f T i + \phi + \theta_i)\} + n_i \quad 0 \leq i < L \quad (26)$$



K = Rician Fade Factor in dB

Fig. 4. GMR channel model

where a_i and θ_i respectively represents the magnitude and phase of Rician fading, and the other terms are the same as in (1). The performance of the estimator is performed in a logical channel TCH3 (3-timeslot traffic channel) of the GMR system, where $T=42.7\mu s$ and $L=112$ symbols^[9].

Fig. 5 and 6 compare the performance of the proposed estimator with others at an SNR of 10dB in an AWGN channel. It can be seen that the Chuang's scheme (2) and the Bellini's scheme (3) provide a wide operating range, but suffer from poor performance. It can also be seen that the Fitz scheme (6) and the L&R scheme (8) provide good performance. However, the Fitz scheme has some weakness compared to the L&R scheme at some frequency offset range mainly due to the effect of phase ambiguity in the $\arg\{z\}$ function. The performance of the proposed scheme is similar to that of the Fitz scheme. Both the Fitz estimator and the L&R schemes use $2L/3$ for M . It can be seen that the proposed scheme provides an operating range narrower than the Chuang and Bellini schemes. However, it provides a sufficient operating range for the maintenance of frequency synchronization because the frequency offset is reduced to a few Hz after initial synchronization.

Fig. 7 and Fig. 8 depicts the performance of the proposed estimator as a function of SNR in the presence of 10Hz frequency offset in AWGN and Rician channel with $K=12$ dB and 200 Hz

Doppler frequency. It can be seen that the proposed scheme provides performance similar to that of the Fitz and the L&R scheme. However, when the phase difference between the two part of the

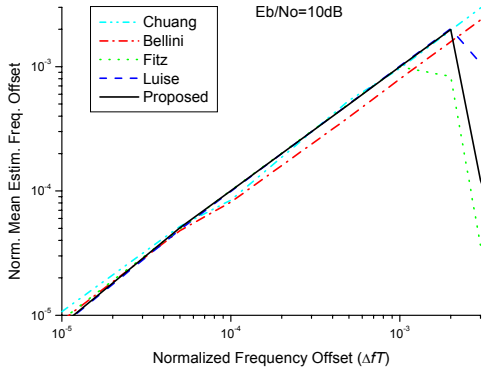


Fig. 5. Averaged performance of the proposed estimation scheme

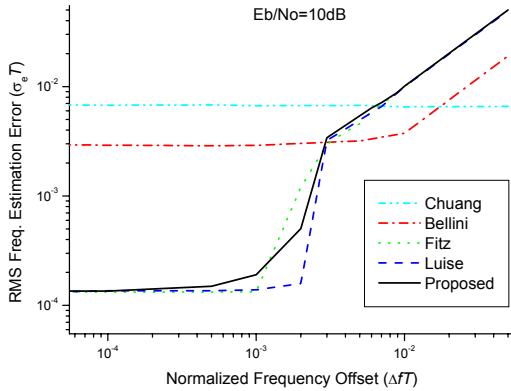


Fig. 6. RMS estimation error of the proposed estimation scheme

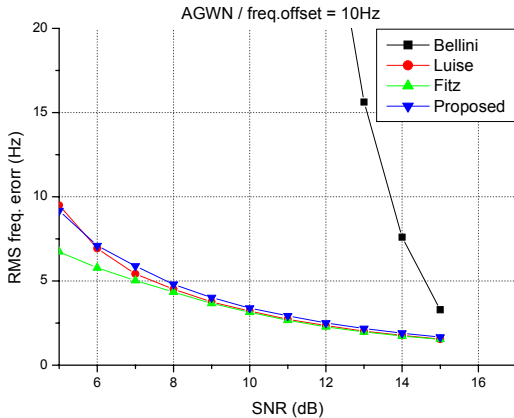


Fig. 7. RMS estimation error in an AWGN channel

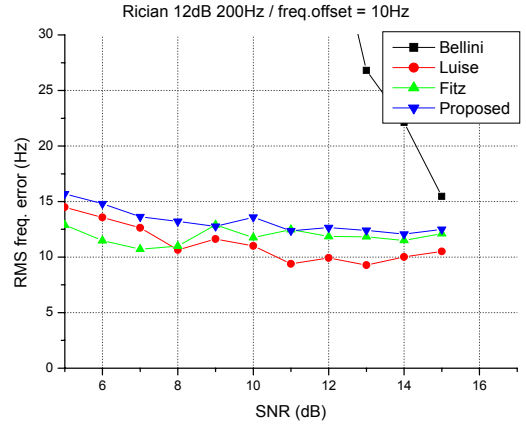


Fig. 8. RMS estimation error in a fading channel

burst is large due to the fading, the proposed scheme may result in a large estimation error. On the other hand, since both the Fitz and the L&R schemes use all the phase difference between the symbols from the autocorrelation function, they can provide performance somewhat robust to frequency offset due to the fading.

Table 1 and Fig. 9 compare the computational complexity of the estimation schemes in consid-

Table 1. Comparison of the implementation complexity

	Opt. value	Real mult.	Real add.
Chuang		$12L-1$	$10L-8$
Bellini	$N = L/2$	L	$L-1$
Fitz	$M = 2L/3$	$16L^2/9-4L/3$	$8L^2/9-2L/3$
Luisse	$M = 2L/3$	$4L^2/3+12L$	$4L^2/3+10L-4$
Proposed	$N = 2L/3$	$8L+4$	$32L/4-3$

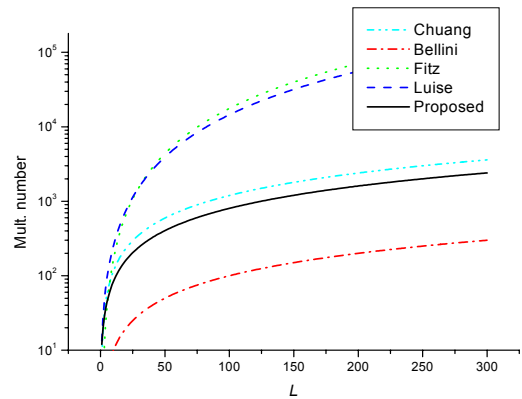


Fig. 9. The comparison of multiplication complexity

eration, where the complexity for the angle calculation of complex symbol with $\arg(\cdot)$ is not included. It can be seen that the proposed scheme significantly reduces the computational complexity compared to other schemes.

IV. Conclusion

In this paper, we have considered the estimation of frequency offset in a TDMA-based satellite system. We have proposed a new non-data aided estimation scheme that estimates the frequency offset based on the difference between the phases of the two parts in the burst. The proposed scheme requires complexity in proportion to the burst length while conventional schemes require complexity in proportion to the square of the burst length. Thus, it can significantly reduce computational complexity, while providing performance similar to conventional schemes. Finally, the performance of the proposed scheme has been analyzed and verified by computer simulation when applied to a GMR system.

REFERENCES

[1] D.J.Goodman, "Trends in Cellular and Cordless communications," *IEEE Commun. Magazine*, vol. 29, pp. 31-40, June 1991.

[2] GSM Recommendation 11.10, Part II.3, V. 1.07.00, Mar. 1990.

[3] GEO-Mobile Radio Interface Specification, Part V.5, V. 1.2.1, April 2002.

[4] C. Heegard, J. A. Heller and A. J. Viterbi, "A Microprocessor-Based PSK Modem for Packet Transmission over Satellite Channels," *IEEE Trans. Commun.*, vol. COM-26, pp. 552-564, May 1978.

[5] M. P. Fitz, "Planar Filtered Techniques for Burst Mode Carrier Synchronization," *IEEE GLOBECOM '91*, Phoenix, AZ, paper 12.1, Dec. 1991.

[6] M. Luise and R. Reggiannini, "Carrier Frequency Recovery in All-Digital Modems for Burst-Mode Transmissions," *IEEE Trans.*

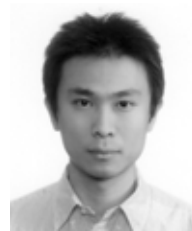
Commun., vol. 43, no. 3, pp. 1169-1178, Mar. 1995.

[7] J. C.-I. Chuang and N. R. Sollenberger, "Burst Coherent Demodulation with Combined Symbol Timing, Frequency Offset Estimation, and Diversity Selection," *IEEE Trans. Commun.*, vol. COM-39, pp. 1157-1164, July 1991.

[8] S. Bellini, C. Molinari and G. Tartara, "Digital Frequency Estimation in Burst Mode QPSK Transmission," *IEEE Trans. Commun.*, vol. 38, pp. 959-961, July 1990.

[9] GEO-Mobile Radio Interface Specification, Part V.2, V. 1.2.1, Apr. 2002.

김 종 문 (Jong-Moon Kim)



정회원

2002년 8월 서울대학교 전기공학부 학사

2004년 8월 서울대학교 전기컴퓨터공학부 석사

2004년 9월~현재 LG전자 DTV 연구소 주임연구원

<관심분야> VSB 시스템, OFDM 시스템, 차세대 통신용 신호 처리

이 용 환 (Yong-Hwan Lee)



종신회원

1977년 서울대학교 전기공학과 학사

1980년 한국과학기술원 전기전자공학과 석사

1989년 University of Massachusetts, Amherst, 박사

1980년~1985년 국방과학연구소 선임연구원

1989년~1994년 Principal engineer in Motorola Inc.

1994년~현재 서울대학교 전기공학부 교수

<관심분야> 유/무선 송수신기 설계, 차세대 통신용 신호 처리